Journal of Crystal Growth 420 (2015) 1–5

Contents lists available at ScienceDirect

Journal of Crystal Growth

journal homepage: www.elsevier.com/locate/jcrysgro

The formation of high number density InSb quantum dots, resulting from direct InSb/GaSb (001) heteroepitaxy

J.J. Bomphrey*, M.J. Ashwin, T.S. Jones

Department of Chemistry, University of Warwick, Coventry CV4 7AL, United Kingdom

ARTICLE INFO

Article history:
Received 23 January 2015
Received in revised form
10 March 2015
Accepted 13 March 2015
Communicated by H. Asahi
Available online 23 March 2015

Keywords:
A1. Nanostructures
A1. Semiconducting III–V materials
A3. Molecular beam epitaxy
A3. Antimonides

ABSTRACT

We report the direct deposition of indium antimonide, by molecular beam epitaxy (MBE) on gallium antimonide, resulting in the formation of quantum dots (QDs) with a maximum density of $\sim 5.3 \times 10^{10}$ cm^{-2}. Using reflection high energy electron diffraction (RHEED) and atomic force microscopy (AFM) for the analysis of samples with InSb depositions of 1–6 ML equivalent thickness, we observe an apparent value for the critical thickness for InSb/GaSb (001) deposition of 2.3 ± 0.3 ML, for the growth temperatures of 275 °C and 320 °C.

1. Introduction:

Quantum dots (QDs) have emerged as a prominent area of research in relation to the development of photoemitters and infrared detectors [1–4]. The benefits of quantum confinement, such as a narrow emission line-width and increased differential gain as a function of carrier density have been reported in the InAs/GaAs system [5], suggesting that coupling QD morphology with narrow band gap materials offers promise in the development of emitters in the technologically important mid-IR region.

n-type InSb exhibits a narrow band gap and a small electron effective mass at room temperature [6], making it theoretically suitable in the development of photonic devices. However, difficulties in substrate lattice matching and compositional consistency of InSb derivatives have previously hindered device development [7].

Since the emergence of research concerning MBE grown self-assembled InSb QDs in 1996 [7,8], there has been increasing interest in relation to optoelectronic and ultrafast device applications [2,6,9–11]. Thought to exhibit thermally stable emission characteristics [4], InSb QDs offer the prospect of detector and laser diode operation [1] in the 3–5 μm region of the electromagnetic spectrum, with 3.8 μm emission (300 K) having been reported previously for MBE-grown InSb QDs on InAs (001) [2].

Formed via Stranski–Krastanov (SK) growth, due to a lattice mismatch of ca. 6.4% with GaSb, there are similarities between InSb/GaSb (001) growth and the InAs/GaAs (001) heteroepitaxial system [12,13], which has been extensively documented [12,14–19]. In the latter, strain-driven QD formation is observed after deposition of a critical thickness of InAs (~1.6 ML) [12,20–23], after which accumulated strain energy in the material leads to preferential formation of islands. There are, however, some important differences, for example the low bond energy of InSb [24], in which case one might expect a larger critical thickness than that reported for InAs/GaAs [4,19,25].

Unlike the InAs/GaAs system, factors such as the increased diffusion length of indium on Sb-terminated surfaces [4] due to the lower In-Sb bond energy, and the surfactant properties of Sb [26,27] have accounted for low QD densities (10^9 cm^{-2}) [4], with defect formation serving to reduce the power density/sensitivity for device applications [28].

In this work, we report the formation of a high number density of QDs, without the requirement of post-growth annealing or group V exchange, and the present analysis of the InSb/GaSb critical thickness.

2. Experimental

Sample growth was conducted in a GEN II MBE system, with a base pressure $< 2 \times 10^{-10}$ Torr. The system is equipped with SUMO-type group III sources and a valved cracker (Addon) supplying an Sb_2 flux.

* Corresponding author.
E-mail address: J.J.Bomphrey@Warwick.ac.uk (J.J. Bomphrey).

http://dx.doi.org/10.1016/j.jcrysgro.2015.03.025

For each growth, a quarter of an undoped 2" GaSb (001) wafer was mounted on an indium-free platen. Following outgassing at 300 °C, the substrates were admitted to the growth chamber, where the oxide layer was thermally removed (~550 °C) under a stabilising Sb_2 flux (~2×10^{-6} Torr). The substrate temperature, T_{sub}, was determined by pyrometry. A 100 nm GaSb buffer layer was then grown on the substrate (0.5 μm h^{-1}, 500 °C < T_{sub} < 520 °C), to achieve a planar surface, after which the substrate temperature was immediately reduced to the desired growth temperature (275 °C or 320 °C). The surface was stabilised with an incident Sb_2 flux, until the substrate temperature fell below 370 °C. Following a period of time to allow thermal equilibration of the substrate, InSb growth commenced at a rate of 0.1 ± 0.01 MLs^{-1} and a V:III of ~1.2:1. RHEED video was recorded in the $[\bar{1}10]$ direction, for analysis, during deposition.

Surface topography was determined by AFM, in tapping mode, by use of an MFP-3D instrument (Asylum Research), with quantitative topographic analysis undertaken through the Asylum Research software.

3. Results and discussion

The recorded RHEED patterns (Fig. 1) show the evolution of the surface, from the 5x surface reconstruction of the GaSb (001) surface, to a symmetric 3x reconstruction immediately upon the commencement of InSb deposition. RHEED oscillations were also observed and recorded during the initial stages of growth and prior to 3D island formation, confirming the InSb deposition rate.

While InSb is reported to exhibit either an asymmetric (1×3) or a $c(4 \times 4)$ pattern [29,30] at normal growth temperatures, a symmetric (1×3) reconstruction would be observed for a growing GaSb surface and implies a strained InSb layer. A spotted pattern, after some quantity of InSb deposition, was taken as indicative that 3D surface features had been formed [31]. This was subsequently confirmed by AFM. The lack of chevrons in the spot pattern is in contrast to RHEED observations on both InAs/GaAs (001) (quantum dot) [32] and InAs/InP (001) (quantum wire) growth [33], where chevrons have been observed in each case. This implies that there are no sufficiently large planar facets to produce chevron features [34]. After the onset of 3D island formation, a streaked pattern remained visible, thought to result from inter-island planar regions.

The spacing between the specular spot and the first order Bragg spot was also observed to decrease, indicating an increase in the lateral lattice parameter, consistent with a transition from pseudomorphic InSb/GaSb growth to relaxed InSb growth (Fig. 2). This is consistent with previous observations for InSb/GaSb growth [7], with the exception that the change was observed here in the RHEED streaks, rather than the transmission spots.

Using the Asylum Research analysis software, dot parameters such as diameter, height and density were established by a height threshold masking method in which a dot perimeter was established, permitting topographic and volumetric analyses to be performed on the *x*, *y* and *z* data therein.

AFM analysis of the grown samples corroborates the observations derived from examination of RHEED patterns, with 3D features observed above a critical deposition thickness. AFM topographs revealed the appearance and evolution of these features, as a function of InSb deposition (Fig. 3), showing no islands after 2 ML InSb deposition, then 3D islands appearing in the scan corresponding to 2.5 ML InSb, consistent with RHEED observations, and enlarging with further deposition. From appearance in the 2.5 ML image until the image of the sample corresponding to 5 ML InSb deposition, the islands range between 10 and 60 nm equivalent diameter

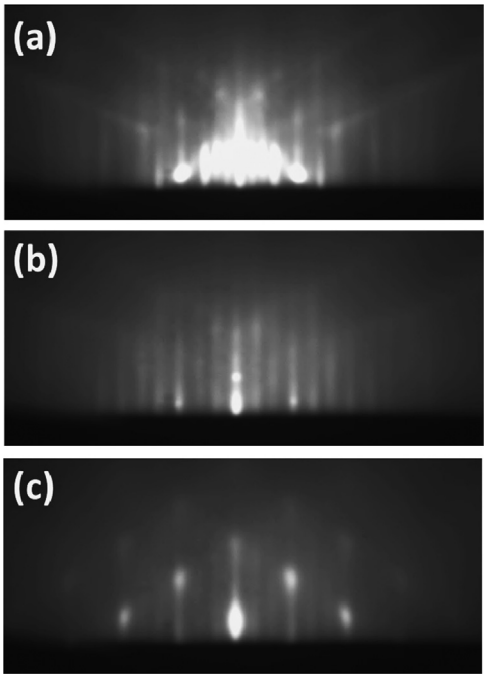

Fig. 1. 13 keV RHEED patterns acquired during the deposition of 3.5 ML InSb on GaSb (001), at 275 °C, and in the $[\bar{1}10]$ azimuth. At zero deposition, the 5-fold reconstruction of Sb-rich GaSb (001) is visible (a), with a sharp transition to a 3-fold pattern upon InSb deposition (b). The spotted pattern visible in (c) indicates a transition from 2D to a surface with 3D features.

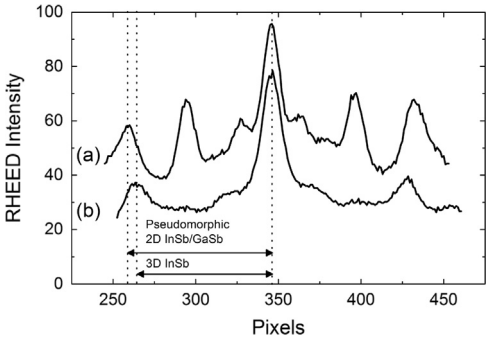

Fig. 2. RHEED line scans after (a) < 1 ML and (b) 3.5 ML equivalent deposition thicknesses of InSb, indicating an increase in the lateral lattice spacing.

(*d*) and are of the order of 2–6 ML (1.3–3.9 nm) in height (*h*). These figures provide an aspect ratio (*h*/*d*) for the 3D islands within the range $0.02 < h/d < 0.13$, comparable with aspect ratios reported for InAs/InP [28], InAs/GaAs [14] and InSb/GaSb [4].

For both growth temperatures, 3D island density was observed to peak rapidly after the critical thickness of InSb had been deposited. A sharper rise and higher island density was observed for the samples grown at 275 °C, than for 320 °C, with both growth temperatures displaying ripening and a degree of island coalescence. Correspondingly, a decrease in number density upon further material deposition was observed (Fig. 4).

Analysis of the dot density as a function of InSb deposition yielded a peak value of 5.3×10^{10} cm^{-2} after deposition of ~3 ML at 275 °C and 3.5×10^{10} cm^{-2} after ~4 ML InSb at 320 °C. These values exceed those reported previously for direct MBE (7×10^{8} cm^{-2}) [1] or MOVPE (~10^{9} cm^{-2}) growth [3] and are comparable with that observed for InAs/GaAs 3D island density and in the work of Tasco et al. concerning InSb/GaSb, after annealing (7×10^{10} cm^{-2}) [4]. The post-growth annealing stage in the latter study was designed to improve the density and

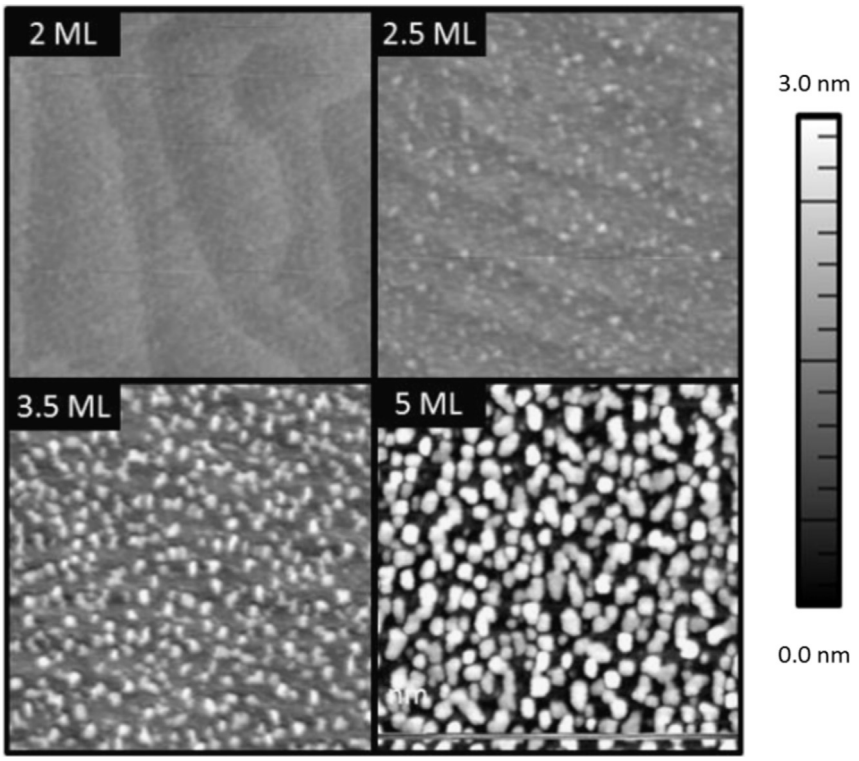

Fig. 3. $1 \times 1\ \mu m^2$ AFM scans, demonstrating surface topography after the deposition of an indicated quantity of InSb at 275 °C. The height data range for each image corresponds to the bar shown.

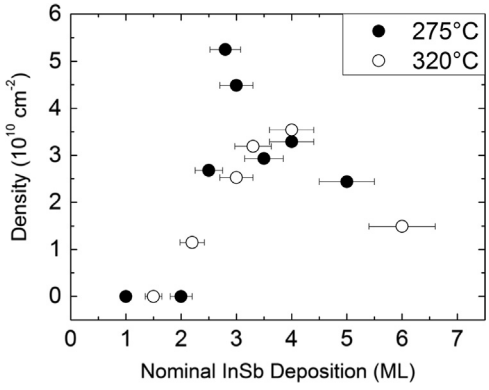

Fig. 4. A plot of 3D island density as a function of InSb deposition for each growth temperature.

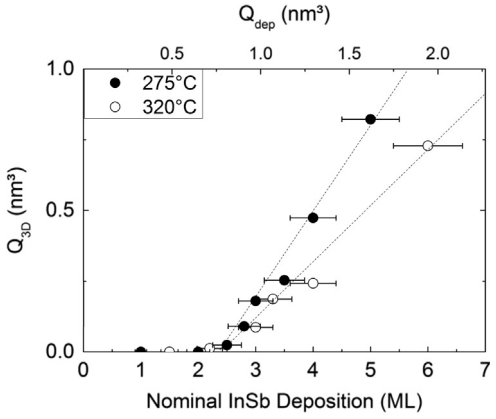

Fig. 5. A plot of 3D island volume as a function of material deposition.

physical properties of the QDs [4], although critical thickness and more detailed analysis were unreported. In this study, there was no evidence of wire structures preceding the onset of dot formation, as observed for InAs/InP, possibly due to the lack of anion exchange [35].

Whilst a critical thickness of ~2 ML may be inferred from Fig. 4, it is more useful to consider the observed total volume of the 3D islands and the amount of InSb deposited: since, in SK growth, island formation occurs atop a wetting layer, it is expected that there should be no islands until after the critical thickness is reached. This can be written, assuming that the wetting layer volume remains unchanged, as

$$Q_{3D} = Q_{dep} - Q_{2D} \quad (1)$$

where Q_{3D} is the volume observed within islands per square nanometre, Q_{dep} is the volume of InSb supplied to the surface per square nanometre and Q_{2D} is the volume contributing to 2D growth in the wetting layer per square nanometre and is proportional to the deposition thickness of InSb. This allows an extrapolation to the amount of InSb deposition at which onset of island growth is observed. A plot of 3D island volume as a function of nominal deposition thickness permits such an extrapolation (Fig. 5), with the x-intercepts of the lines at 2.3 ML indicating the critical thickness of the 2D InSb/GaSb wetting layer.

The obtained value of 2.3 ± 0.3 ML is similar to that obtained by Bertru et al. at 380 °C (~2.3 ML) [7] and appears to be unchanged for the substrate temperatures used here. This apparent temperature insensitivity is also reported for InAs/GaAs (001) growth, where the critical thickness was demonstrated to be constant over a range greater than 100 °C [19], with the previously reported temperature dependence of InAs/GaAs critical thickness [36] being attributed instead to indium re-evaporation above 500 °C [19]. Since the temperatures used here are well below those at which the indium sticking coefficient varies, the consistency of the critical thickness values determined is unsurprising. It is thought

that the larger value of critical thickness for InSb/GaSb, in comparison to InAs/GaAs, is due to the larger Sb atom and, in comparison with InAs, the lower InSb binding energy resulting in a film better able to accommodate strain during growth [4]. Combined with the amount of bond distortion, this correlates with the InSb/GaSb (001) critical thickness lying between that of InAs/GaAs (001) [12] and InAs/InP (001) [35].

While the x-intercepts in Fig. 5 are consistent, the gradients of the trends for each of the two growth temperatures differ, indicating that the rate of increase of the volume of material in the 3D islands as a function of InSb deposition is lower at a growth temperature of 320 °C, compared with that at 275 °C.

Examination of the evolution of Q_{2D} for each series was achieved by rearranging Eq. (1), providing a plot of Q_{2D} as a function of the volume of InSb deposition (Fig. 6) according to

$$Q_{2D} = Q_{dep} - Q_{3D} \tag{2}$$

For the samples grown at 275 °C, the deviation from the initial linearity as dots are formed tends toward a plateau of Q_{2D} with increasing InSb deposition. This is consistent with further growth contributing predominantly to the islands and may be justified as follows: since for $Q_{dep} < Q_c$, where Q_c is the critical volume deposited per nm^2, the Q_{3D} term is equal to zero, giving

$$Q_{2D} = Q_{dep} \tag{3}$$

which has a gradient of 1.

For the case of $Q_{dep} > Q_c$, where island growth dominates, (2) gives

$$\frac{dQ_{2D}}{dQ_{dep}} = 1 - \frac{dQ_{3D}}{dQ_{dep}} \tag{4}$$

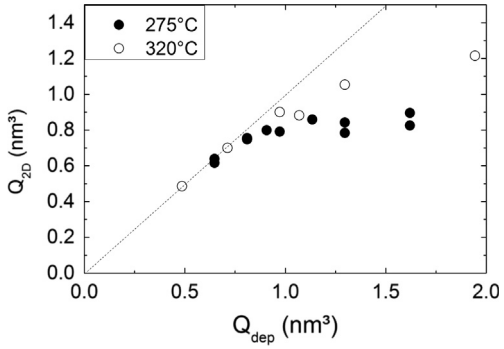

Fig. 6. A plot of Q_{2D} as a function of Q_{dep}, indicating a difference in trend between the series grown at 275 °C versus that which was grown at 320 °C.

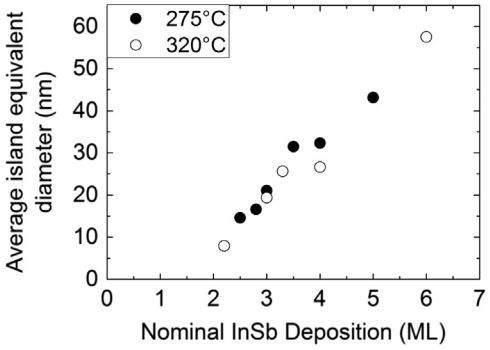

Fig. 7. A plot of 3D island circular-equivalent diameter, as a function of InSb deposition.

Since, after Q_c is achieved, the rates of increase of Q_{dep} and Q_{3D} are the same and, assuming no change in the wetting layer thickness, Eq. (4) becomes

$$\frac{dQ_{2D}}{dQ_{dep}} = 0 \tag{5}$$

corresponding to a plateau with respect to increasing InSb deposition.

While the data from the samples grown at 320 °C do deviate from the linear trend, they do not plateau within the deposition quantities probed. This suggests that some indium is unaccounted for, as the Q_{2D} continues to increase with increasing deposition, indicative of material that is not considered in the analysis. The temperature employed here is too low for the onset of In re-evaporation [7,37], however, requiring another explanation.

Another possibility is group III intermixing at the InSb/GaSb interface. In such a situation, it is expected the formation of $In_xGa_{1-x}Sb$ and accompanying reduction in layer strain, would lead to a larger critical thickness [36]. However, since intermixing has been shown to have a strong dependence upon temperature, this scenario is thought to be unlikely, as there is no observed difference in the critical thickness for the temperatures studied here.

Completed layers of InSb form the surface from which the dot dimensions are referenced and so do not contribute to the volume determined by AFM. Therefore, deposited InSb that completes 2D growth would not be accounted for. This has previously been observed for InAs/GaAs (001) [14], and may be explained by a higher substrate temperature facilitating adatoms deposited on top of a QD to overcome the energy barriers involved in migrating away from the island. Additionally, the limitations of AFM as a technique may not successfully detect incomplete inter-island, 2D growth of a monolayer in height.

In examination of the evolution of island diameter with respect to InSb deposition (Fig. 7), there is no discernable evidence of wide scale coalescence, which would lead to a significant increase in measured island diameter when the mean island diameter and mean inter-centroid distance of island bases coincide. Instead, we suggest that the increase in island diameter is attributable to a combination of increased material deposition and Ostwald ripening [38]. In addition, the diameter of the islands was not observed to vary significantly between growth temperatures (Fig. 7), indicating that it is the difference in the rates of increase of island height that accounts for the difference in the rate of island volume increase. The data suggest that the indium previously unaccounted for participates in 2D growth between islands, completing additional layers, with 3D growth continuing atop, thus causing the ongoing increase in Q_{2D} observed for the samples grown at 320 °C. This is further supported by the observed difference in vertical island growth rate for the two growth temperatures (Fig. 8), indicating that the higher growth temperature facilitates greater

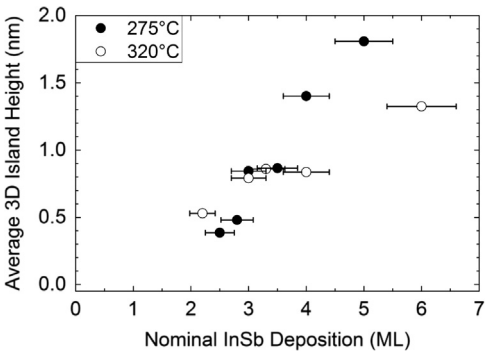

Fig. 8. A plot of average 3D island height as a function of InSb deposition.

adatom mobility and favours the formation of shorter islands. This results in QDs of a lower aspect ratio as InSb deposition continues.

4. Conclusions

We demonstrate that formation of QDs can be achieved by direct deposition of InSb onto GaSb (001), at a high number density ($5.25 \times 10^{10}\,cm^{-3}$) without the requirement for post-growth annealing. A value for the critical thickness of QD formation for the InSb/GaSb (001) system is found to be 2.3 ± 0.3 ML.

The apparent discrepancy between the volume of material deposited and that which was observed for the samples grown at the elevated temperature is explained by growth between the islands, forming completed layers.

Acknowledgements

The authors would like to acknowledge support from the UK Engineering and Physical Sciences Research Council (EPSRC) (Grant number: EP/F041160/1).

References

[1] S. Shusterman, Y. Paltiel, a. Sher, V. Ezersky, Y. Rosenwaks, High-density nanometer-scale InSb dots formation using droplets heteroepitaxial growth by MOVPE, J. Cryst. Growth 291 (2006) 363–369. http://dx.doi.org/10.1016/j.jcrysgro.2006.03.042.
[2] P.J. Carrington, V.A. Solov'ev, Q. Zhuang, S.V. Ivanov, A. Krier, InSb quantum dot LEDs grown by molecular beam epitaxy for mid-infrared applications, Microelectron. J. 40 (2009) 469–472. http://dx.doi.org/10.1016/j.mejo.2008.06.058.
[3] P. Möck, G.R. Booker, N.J. Mason, R.J. Nicholas, E. Aphandéry, T. Topuria, et al., MOVPE grown self-assembled and self-ordered InSb quantum dots in a GaSb matrix assessed by AFM, CTEM, HRTEM and PL, Mater. Sci. Eng. B 80 (2001) 112–115. http://dx.doi.org/10.1016/S0921-5107(00)00625-5.
[4] V. Tasco, N. Deguffroy, A.N. Baranov, E. Tournié, B. Satpati, A. Trampert, et al., High-density InSb-based quantum dots emitting in the mid-infrared, J. Cryst. Growth 301-302 (2007) 713–717. http://dx.doi.org/10.1016/j.jcrysgro.2006.09.016.
[5] T.C. Newell, D.J. Bossert, A. Stintz, B. Fuchs, K.J. Malloy, L.F. Lester, Gain and linewidth enhancement factor in InAs quantum-dot laser diodes, IEEE Photonics Technol. Lett. 11 (1999) 1527–1529. http://dx.doi.org/10.1109/68.806834.
[6] S. Vishwakarma, Study of structural property of n-type indium antimonide thin films, Indian J. Pure Appl. Phys. 50 (2012) 339–346.
[7] N. Bertru, O. Brandt, M. Wassermeier, K. Ploog, Growth mode, strain relief, and segregation of (Ga,In) Sb on GaSb (001) grown by molecular beam epitaxy, Appl. Phys. Lett. 68 (1996) 31. http://dx.doi.org/10.1063/1.116746.
[8] B.R. Bennett, R. Magno, B.V. Shanabrook, Molecular beam epitaxial growth of InSb, GaSb, and AlSb nanometer-scale dots on GaAs, Appl. Phys. Lett. 68 (1996) 505. http://dx.doi.org/10.1063/1.116381.
[9] D.L. Partin, J. Heremans, C.M. Thrush, Indium antimonide doped with manganese grown by molecular beam epitaxy, J. Cryst. Growth 175-176 (1997) 860–867. http://dx.doi.org/10.1016/S0022-0248(96)00916-5.
[10] D.L. Partin, J. Heremans, C.M. Thrush, Growth and characterization of indium antimonide doped with lead telluride, J. Appl. Phys. 71 (1992) 2328. http://dx.doi.org/10.1063/1.351106.
[11] S. Ivanov, A. Boudza, R. Kutt, N.N. Ledentsov, B.Y. Meltser, S.S. Ruvimov, et al., Molecular beam epitaxial growth of InSb/GaAs (100) and InSb/Si (100) heteroepitaxial layers (thermodynamic analysis and characterization), J. Cryst. Growth 156 (1995) 191–205. http://dx.doi.org/10.1016/0022-0248(95)00305-3.
[12] T.J. Krzyzewski, P.B. Joyce, G.R. Bell, T.S. Jones, Wetting layer evolution in InAs/GaAs (001) heteroepitaxy: effects of surface reconstruction and strain, Surf. Sci. 517 (2002) 8–16. http://dx.doi.org/10.1016/S0039-6028(02)02083-6.
[13] M. Rosini, M. Righi, P. Kratzer, R. Magri, Indium surface diffusion on InAs (2×4) reconstructed wetting layers on GaAs (001), Phys. Rev. B 79 (2009) 075302. http://dx.doi.org/10.1103/PhysRevB.79.075302.
[14] P. Howe, E.C. Le Ru, E. Clarke, R. Abbey, R. Murray, T.S. Jones, Competition between strain-induced and temperature-controlled nucleation of InAs/GaAs quantum dots, J. Appl. Phys. 95 (2004) 2998. http://dx.doi.org/10.1063/1.1645637.
[15] P. Howe, B. Abbey, E.C. Le Ru, R. Murray, T.S. Jones, Strain-interactions between InAs/GaAs quantum dot layers, Thin Solid Films 464-465 (2004) 225–228. http://dx.doi.org/10.1016/j.tsf.2004.06.055.
[16] F. Bastiman, A.G. Cullis, M. Hopkinson, InAs/GaAs (001) molecular beam epitaxial growth in a scanning tunnelling microscope, J. Phys. Conf. Ser. 209 (2010) 012048. http://dx.doi.org/10.1088/1742-6596/209/1/012048.
[17] T. Krzyzewski, P. Joyce, G. Bell, T. Jones, Role of two- and three-dimensional surface structures in InAs-GaAs (001) quantum dot nucleation, Phys. Rev. B 66 (2002) 121307. http://dx.doi.org/10.1103/PhysRevB.66.121307.
[18] T.J. Krzyzewski, T.S. Jones, Ripening and annealing effects in InAs/GaAs (001) quantum dot formation, J. Appl. Phys. 96 (2004) 668. http://dx.doi.org/10.1063/1.1759788.
[19] F. Patella, F. Arciprete, M. Fanfoni, A. Balzarotti, E. Placidi, Apparent critical thickness versus temperature for InAs quantum dot growth on GaAs (001), Appl. Phys. Lett. 88 (2006) 161903. http://dx.doi.org/10.1063/1.2189915.
[20] E. Placidi, F. Arciprete, R. Magri, M. Rosini, A. Vinattieri, L. Cavigli, et al., Self-Assembly of Nanostructures, Springer, New York, New York, NY (2012) http://dx.doi.org/10.1007/978-1-4614-0742-3.
[21] D. Leonard, K. Pond, P. Petroff, Critical layer thickness for self-assembled InAs islands on GaAs, Phys. Rev. B 50 (1994) 11687–11692. http://dx.doi.org/10.1103/PhysRevB.50.11687.
[22] J.A. Venables, G.D.T. Spiller, M. Hanbucken, Nucleation and growth of thin films, Rep. Prog. Phys. 47 (1984) 399–459. http://dx.doi.org/10.1088/0034-4885/47/4/002.
[23] P.B. Joyce, T.J. Krzyzewski, G.R. Bell, T.S. Jones, Surface morphology evolution during the overgrowth of large InAs–GaAs quantum dots, Appl. Phys. Lett. 79 (2001) 3615. http://dx.doi.org/10.1063/1.1420579.
[24] F. Hatami, S.M. Kim, H.B. Yuen, J.S. Harris, InSb and InSb:N multiple quantum dots, Appl. Phys. Lett. 89 (2006) 133115. http://dx.doi.org/10.1063/1.2357546.
[25] T.J. Krzyzewski, P.B. Joyce, G.R. Bell, T.S. Jones, Understanding the growth mode transition in InAs/GaAs (001) quantum dot formation, Surf. Sci. 532-535 (2003) 822–827. http://dx.doi.org/10.1016/S0039-6028(03)00455-2.
[26] T.J. Garrod, J. Kirch, P. Dudley, S. Kim, L.J. Mawst, T.F. Kuech, Narrow band gap GaInNAsSb material grown by metal organic vapor phase epitaxy (MOVPE) for solar cell applications, J. Cryst. Growth 315 (2011) 68–73. http://dx.doi.org/10.1016/j.jcrysgro.2010.08.010.
[27] E. Tournié, K.H. Ploog, Surfactant-mediated molecular beam epitaxy of strained layer semiconductor heterostructures, Thin Solid Films 231 (1993) 43–60. http://dx.doi.org/10.1016/0040-6090(93)90702-Q.
[28] Q. Zhuang, S. Yoon, H. Zheng, K. Yuan, Growth of self-organized InAs quantum dots on InP by solid-source molecular beam epitaxy, J. Cryst. Growth 216 (2000) 57–61. http://dx.doi.org/10.1016/S0022-0248(00)00375-4.
[29] R. Droopad, R.L. Williams, S.D. Parker, RHEED intensity oscillations observed during the MBE growth of InSb (100), Semicond. Sci. Technol. 4 (1989) 111–113. http://dx.doi.org/10.1088/0268-1242/4/2/009.
[30] C. McConville, T. Jones, F. Leibsle, S. Driver, T. Noakes, M. Schweitzer, et al., Surface reconstructions of InSb (100) observed by scanning tunneling microscopy, Phys. Rev. B 50 (1994) 14965–14976. http://dx.doi.org/10.1103/PhysRevB.50.14965.
[31] G. Balakrishnan, J. Tatebayashi, A. Khoshakhlagh, S.H. Huang, A. Jallipalli L.R. Dawson, et al., III/V ratio based selectivity between strained Stranski–Krastanov and strain-free GaSb quantum dots on GaAs, Appl. Phys. Lett. 89 (2006) 161104. http://dx.doi.org/10.1063/1.2362999.
[32] B. Joyce, D. Vvedensky, Quantum Dots: Fundamentals, Applications, and Frontiers, Springer-Verlag, Berlin/Heidelberg (2005) http://dx.doi.org/10.1007/1-4020-3315-X.
[33] H.R. Gutiérrez, M.A. Cotta, M.M.G. de Carvalho, Faceting evolution during self-assembling of InAs/InP quantum wires, Appl. Phys. Lett. 79 (2001) 3854. http://dx.doi.org/10.1063/1.1424476.
[34] E.M. Clarke, R. Murray, Optical properties of In(Ga)As/GaAs quantum dots for optoelectronic devices, in: M. Henini (Ed.), Handb. Self Assem. Semicond. Nanostructures Nov. Devices Photonics Electron., First, Elsevier, Oxford, 2008, p. 85.
[35] H.J. Parry, M.J. Ashwin, T.S. Jones, InAs nanowire formation on InP (001) J. Appl. Phys. 100 (2006) 114305. http://dx.doi.org/10.1063/1.2399326.
[36] C. Heyn, Critical coverage for strain-induced formation of InAs quantum dots, Phys. Rev. B 64 (2001) 165306. http://dx.doi.org/10.1103/PhysRevB.64.165306.
[37] M. Yata, Growth kinetics of InSb thin films on Si (100) surfaces by In1 and Sb4 molecular beams, Thin Solid Films 137 (1986) 79–87. http://dx.doi.org/10.1016/0040-6090(86)90196-3.
[38] J. Drucker, Coherent islands and microstructural evolution, Phys. Rev. B 48 (1993) 18203–18206. http://dx.doi.org/10.1103/PhysRevB.48.18203.